5.6. Barrow, Alaska (01/14/13 – 11/28/13)

This section describes quality control of solar data recorded at Barrow between 01/14/13 – 11/28/13. A site visit took place between 6/12/13 and 6/17/13 during which the instrument's shutter was upgraded and the instrument was characterized and calibrated. A total of 14,056 scans of the SUV-100 spectroradiometer are part of the Barrow Volume 23 dataset.

As part of the site visit, the system's PSP pyranometer (S/N 27374F3) was replaced by a refurbished pyranometer (S/N 28119F3), which had recently been calibrated by the Eppley Laboratory. Likewise, the system's TUVR radiometer (S/N 27329) was also replaced by a refurbished instrument (S/N 27989). When data were processed with the most recent calibration factor of the new TUVR established by Eppley Laboratory, it was found that the instrument's solar measurements were low by approximately 25% compared to historical TUVR measurements and those of the SUV-100 spectrometer. The calibration factor was adjusted such that TUVR data collected after 6/17/13 are consistent with historical TUVR measurements as well as UV-A (320 - 400 nm) data of the SUV-100. Measurements of the two PSP pyranometers using their most recent calibration factors are consistent and no adjustment was applied.

Data of the SUV-100 spectroradiometer collected during the reporting period were affected by the following problems:

- Reduced duty cycle up to 6/12/13
  When measuring four scans per hour, the system's shutter would not always completely open. To prevent this from occurring, the system's duty cycle had to be reduced to two scans per hour. A new state-of-the-art shutter was designed and tested in 2012 and the system was retrofitted with the new device during the site visit in 2013.
- Misaligned calibration equipment
  When the calibration equipment was inspected at the beginning of the site visit, it was discovered that two legs of the "lamp stand" used to mount the lamp atop the instrument were unfastened resulting in lamps being too far from the instrument's irradiance collector by 4 mm. A distance of 4 mm at a nominal distance of 500 mm leads to a systematic error in the lamp irradiance of 1.6%. It could not be determined when the problem first occurred. Hence, all calibration measurements performed in 2013 up to 6/12/13 were scaled by 1.6%.
- Reduced system sensitivity due to high temperatures
  Between mid-July and mid-August, the air conditioner of the laboratory where the instrument is located failed. At several days during this period, the temperature in the laboratory became so high that the peltier cooler of the spectroradiometer could no longer keep the system's temperature within its control range. On one occasion, the temperature of the monochromator increased from the nominal temperature of 33 °C to 39 °C, leading to a reduction in the system's responsivity by several percent. Because of temperature fluctuations within short amounts of time, data could not be corrected. Affected periods are indicated in Section 5.6.2 and were flagged in the Version 2 data edition.

5.6.1. Irradiance Calibration

The site irradiance standards of the reporting period were the lamps M-699, 200W009, and 200W042, which were also used in 2012.

Lamp 200W042 was calibrated in June 2007 at BSI with four 1000-Watt FEL lamps provided by the Central UV Calibration Facility (CUCF) at Boulder. This calibration procedure was complicated by the fact that the irradiance scale of the four FEL lamps refers to the detector-based scale of the National Institute of Standards and Technology established in 2000 (NIST2000; Yoon et al., 2002), whereas all solar data of the NSF UVSIMN refer to the source-based NIST scale from 1990 (NIST1990, Walker et al.,

1987). The NIST2000 scale is about 1.3% larger than the NIST1990 scale. Data of certificates issued by CUCF were converted to the NIST1990 scale before the calibration was transferred to the site standard.

Lamps M-699 and 200W009 were originally calibrated by Optronic Laboratories (OL) in March 2001. Both lamps were brought to San Diego in 2007 and recalibrated against lamps 200W028 and 200W022. (Lamp 200W028 is the San Diego site standard; lamp 200W022 is BSI's long-term standard, which preserves the OL scale from March 2001.)

The three lamps were compared to the traveling standard 200W017 at the beginning (6/12/13) and end (6/16/13) of the site visit. On 6/12/13, the calibrations of lamps 200W009 and 200W042 agreed to within ±1.0% with that of the traveling standard (Figure 5.6.1). The difference between the calibrations of lamp M-699 and the travelling standard was slightly worse but still within the range of the uncertainty of calibration standards. The comparison on 6/16/13 led to similar results.

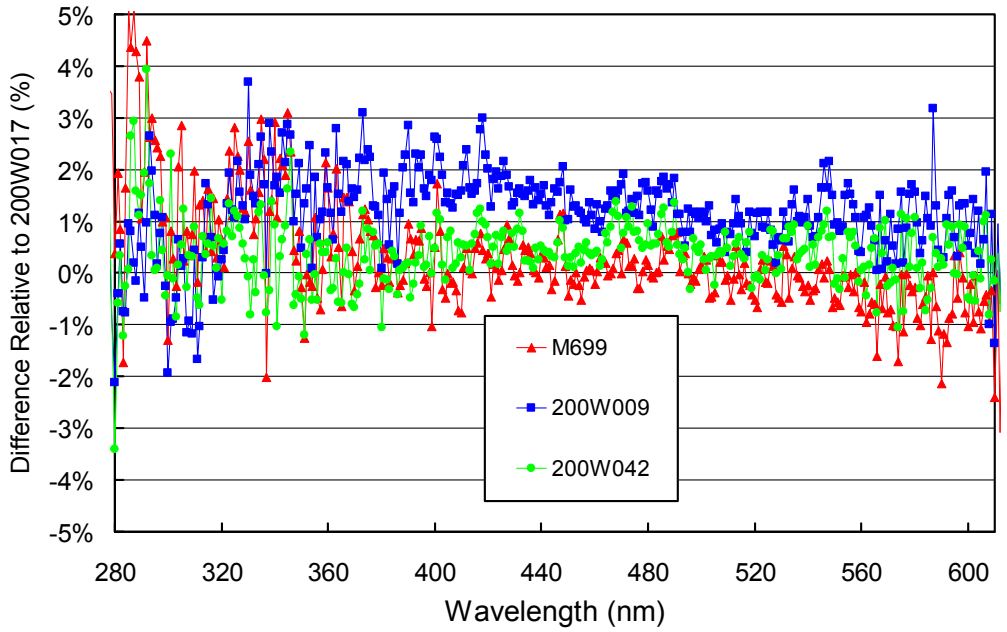

Figure 5.6.1. *Comparison of on-site lamps M-699, 200W009, and 200W042 with traveling standard 200W017 on 6/12/13.*

5.6.2. Instrument Stability and Calibration

The radiometric stability of the SUV-100 spectroradiometer was monitored with calibrations utilizing the three site irradiance standards, daily "response" scans of the internal lamp, by comparison with measurements of the GUV-511 multifilter radiometer, and by comparisons with results of a radiative transfer model.

The stability of the internal lamp is monitored with the TSI sensor, which is independent from possible monochromator and PMT drifts. By logging the PMT currents at several wavelengths during response scans, changes in monochromator throughput and PMT sensitivity can be detected. Figure 5.6.2 shows changes in TSI readings and PMT currents at 300 and 400 nm, derived from response scans performed between 1/1/13 and the beginning of the site visit on 6/12/13. During this time, the output of the internal lamp as indicated by the TSI sensor decreased by less than 1% and this small change is well reflected in the changes of the PMT currents, indicating that monochromator and PMT were stable. After the site visit (Figure 5.6.3), TSI measurements were also consistent, but the PMT current decreased on three occasions

by up to 3% at times when the monochromator temperature was abnormally large. The following periods were affected: 7/16/13 – 7/23/13, 8/2/13 – 8/4/13, and 8/11/13 – 8/13/13. During these periods, the monochromator temperature fluctuated throughout the day as a result of the laboratory's overheating, leading to increased uncertainty in solar data. Affected data periods are indicated in Table 5.6.1 and were flagged in the Version 2 data edition. Magnitudes of systematic errors were estimated from comparison of GUV and SUV data.

Table 5.6.1. Periods with increased uncertainty.

Period	SUV-100 data likely low by	Reason
06/23/13 09:00 – 06/24/13 04:00	10-16%	unknown
06/27/13 17:30 – 06/28/13 04:00	up to 10%	unknown
07/16/13 20:00 – 07/17/13 08:00	up to 8%	overheating
07/20/13 19:00 – 07/22/13 17:00	7-12%	overheating
08/01/13 21:00 – 08/03/13 14:00	up to 10%	overheating
08/11/13 23:00 – 08/12/13 09:00	up to 6%	overheating
08/13/13 00:00 – 08/13/13 04:00	up to 6%	overheating
08/28/13 13: 00 – 08/29/13 05:00	up to 8%	unknown

Through-the-collector calibrations using the site irradiance standards also indicated some variability in system responsivity. To adjust for these small changes, the reporting period was subdivided into four periods. The first period (Period P1) is the period before the site visit when the system was very stable. Figure 5.6.4 shows the ratios of the irradiance assigned to the internal reference lamp in Periods P3 and P4 relative to that applied in Period P2 (the first period after the site visit). Table 5.6.2 provides more information on these periods. The change in responsivity over the year was less than ±3% at all wavelengths.

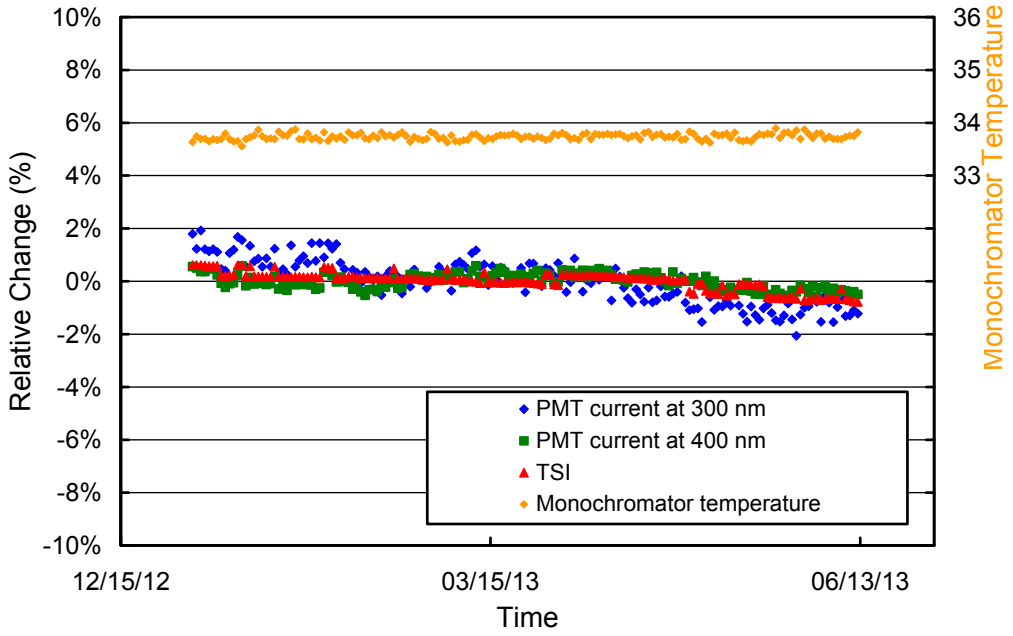

Figure 5.6.2. *Time-series of PMT current at 300 and 400 nm, and TSI signal measured before the site visit. All data were extracted from measurements of the internal irradiance standard and are normalized to their average.*

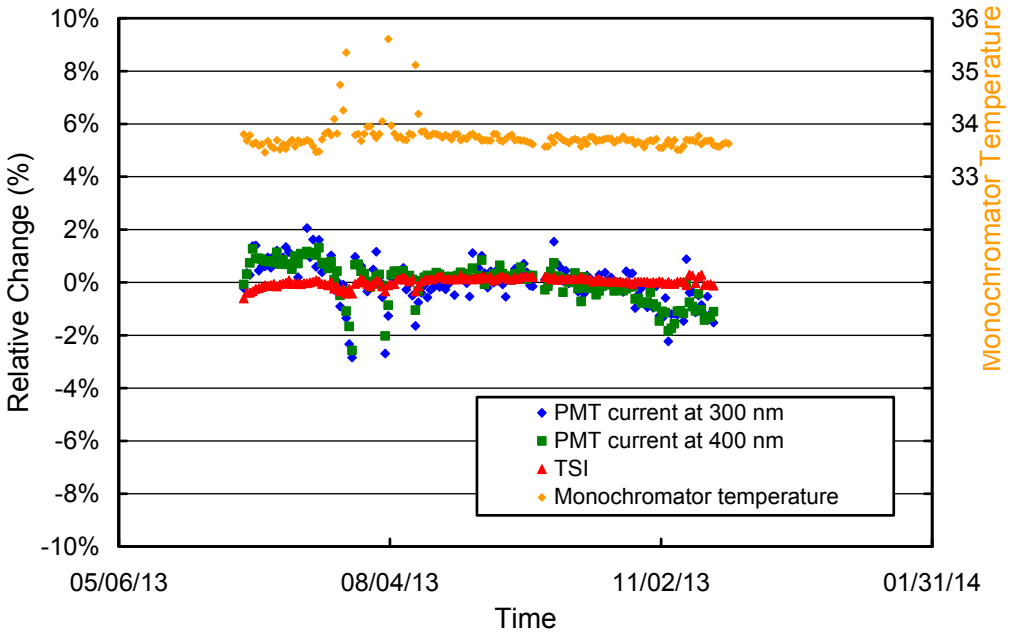

Figure 5.6.3. *Time-series of PMT current at 300 and 400 nm, and TSI signal measured after the site visit. All data were extracted from measurements of the internal irradiance standard and are normalized to their average. Drops in PMT current are apparent at time when the monochromator temperature was elevated.*

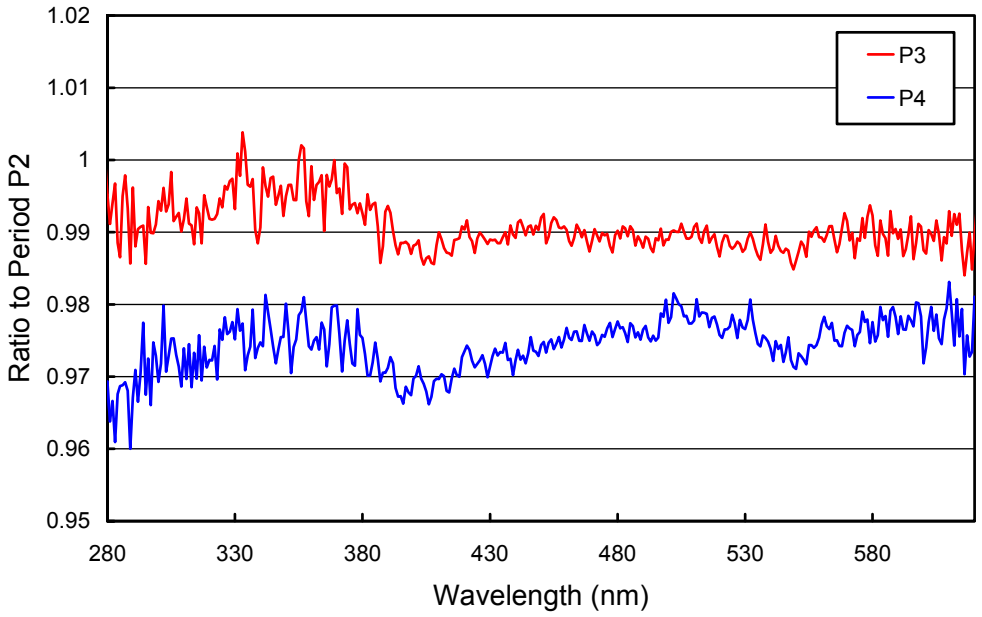

Figure 5.6.4. *Ratios of spectral irradiance assigned to the internal reference lamp during the Periods P3 and P4, relative to Period P2.*

Table 5.6.2. Calibration periods for Barrow Volumes 23.

Period name	Period range	Number of absolute scans
P1	01/01/13 - 06/12/13	11
P2	06/15/13 - 09/21/13	7
P3	09/22/13 - 10/23/13	1
P6	10/24/13 - 12/31/13	5

Figure 5.6.5 presents ratios of standard deviation and average spectra, calculated from individual absolute scans performed in each calibration period. These ratios are useful for estimating the variability of calibrations assigned to each period. The variability is less than 1.5% for all periods.

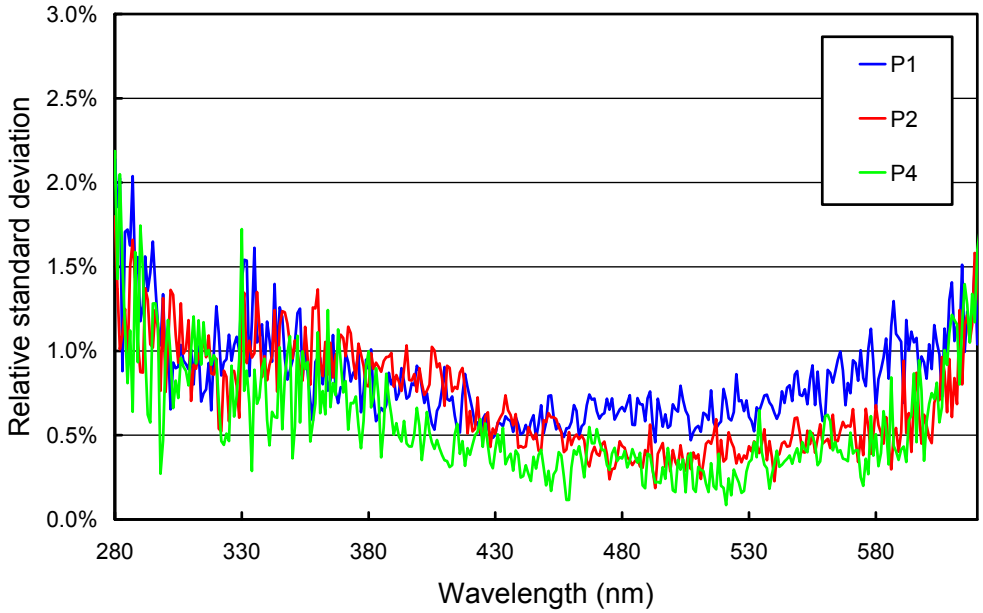

Figure 5.6.5. *Ratio of standard deviation and average spectra calculated from irradiance spectra applied to the internal lamp.*

SUV-100 data were also compared to measurements of the collocated GUV-511 radiometer. The ratio of GUV and SUV data at 320 nm as a function of time is shown in Figure 5.6.6. The standard deviation of the ratio is 0.032. Variability is generally smaller in spring than fall because of less influence by clouds. The GUV/SUV ratio shows several step changes and short periods with systematic (i.e., non-random) difference from one. Periods when SUV measurements were low are listed in Table 5.6.2 and are highlighted with arrows in Figure 5.6.6.

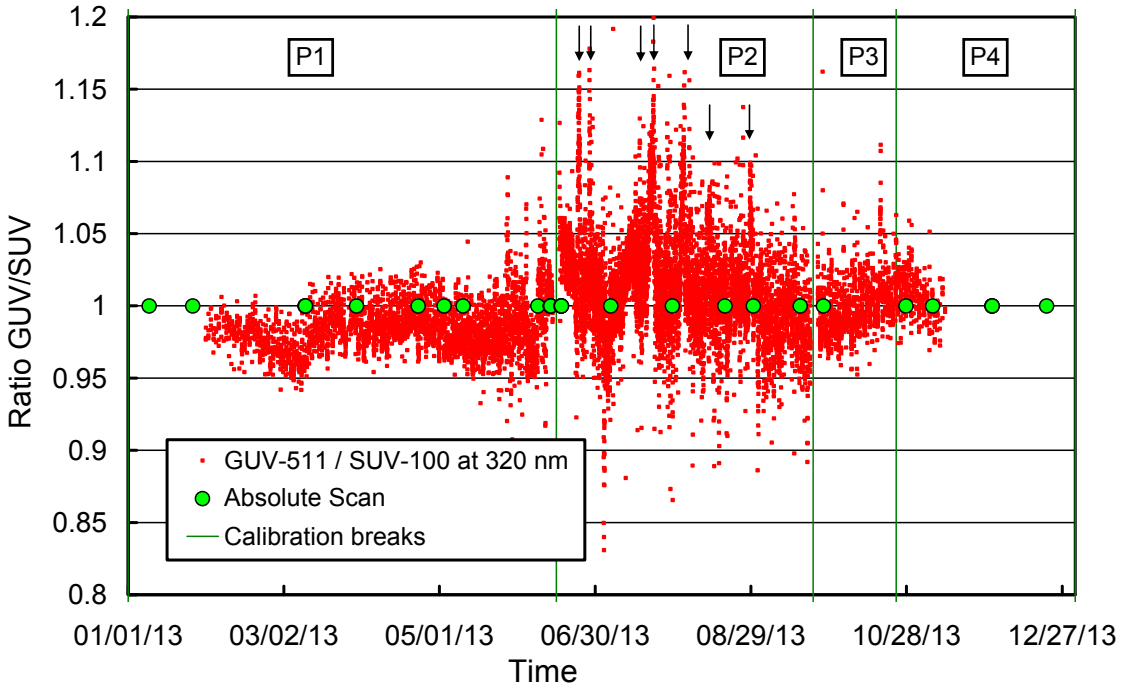

Figure 5.6.6. *Ratio of GUV-511 measurements of the 320-nm channel to SUV-100 measurements. The latter were weighted with the spectral response function of the 320-nm GUV-511 channel. Times of absolute scans and calibration breaks are also indicated. Arrows indicate the periods listed in Table 1 when SUV measurements were low.*

As a last check of data quality, SUV-100 measurements were compared with radiative transfer calculations. These calculations are part of Version 2 processing (uv.biospherical.com/ NSF/Version2/). The ratio of measured and modeled data was generally within the range observed in past years with the exception of the short periods indicated in Table 5.6.2, when measurements tended to be lower than the model results, consistent with the comparison with the GUV.

5.6.3. Wavelength Calibration

Wavelength stability of the system was monitored with the internal mercury lamp. Information from the daily wavelength scans was used to homogenize the data set by correcting day-to-day fluctuations in the wavelength offset. Figure 5.6.7 shows the differences in the wavelength offset of the 296.73 nm mercury line between two consecutive wavelength scans. A total 397 pairs, measured between 1/1/13 and 12/31/13, were evaluated. The change in offset was smaller than ±0.055 nm in 98.5% of all cases. Larger steps were mostly related to site visit activities and operator errors.

Functions for correcting the non-linearity of the monochromator's wavelength drive are shown in Figure 5.6.8. The functions were calculated with the Version 2 Fraunhofer line correlation method (*Bernhard et al*., 2004), separately for the periods before and after the site visit. Data were corrected with these functions and again tested with the correlation method. Results for four wavelengths in the UV and one in the visible are shown in Figure 5.6.9. Residual shifts in the UV are typically smaller than ±0.05 nm. The average standard deviation for all wavelengths between 310 and 590 nm is 0.027 nm. Wavelength errors are slightly larger for the period after the site visit. These errors have been further reduced in the Version 2 data set.

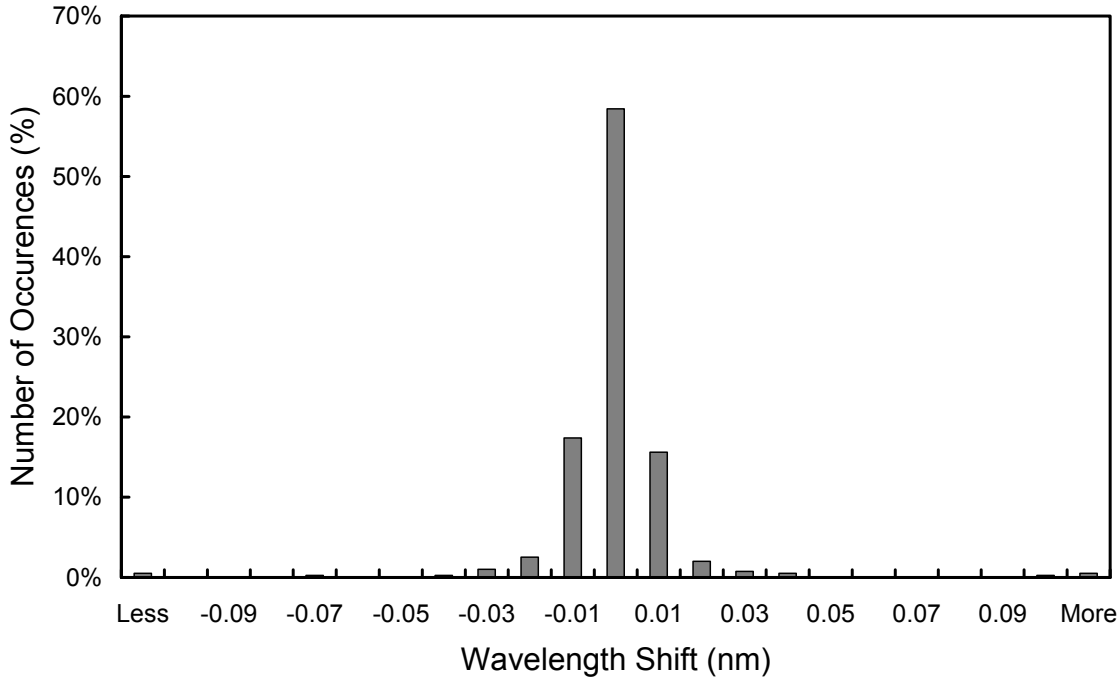

Figure 5.6.7. *Differences in the measured position of the 296.73 nm mercury line between consecutive wavelength scans. The x-labels give the center wavelength shift for each column. Thus the 0-nm histogram column covers the range -0.005 to +0.005 nm. "Less" means shifts smaller than –0.105 nm; "more" means shifts larger than 0.105 nm.*

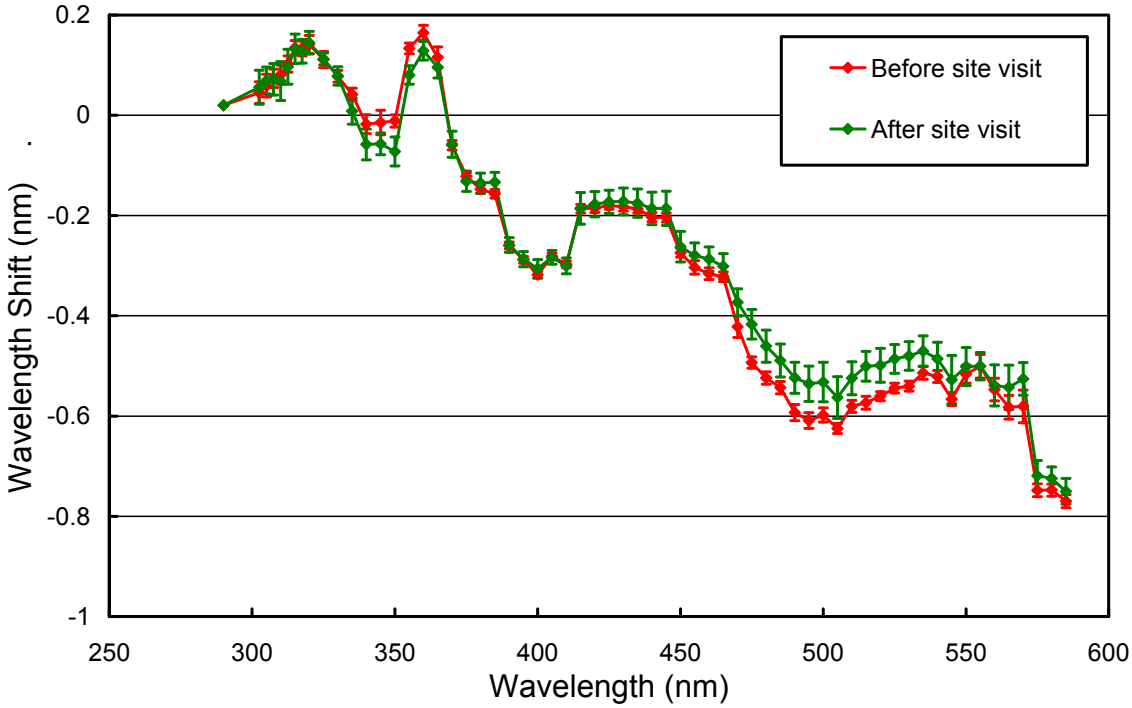

Figure 5.6.8. *Monochromator non-linearity correction functions for Barrow Volume 23. Error bars indicate the standard deviation of the data contributing to this plot.*

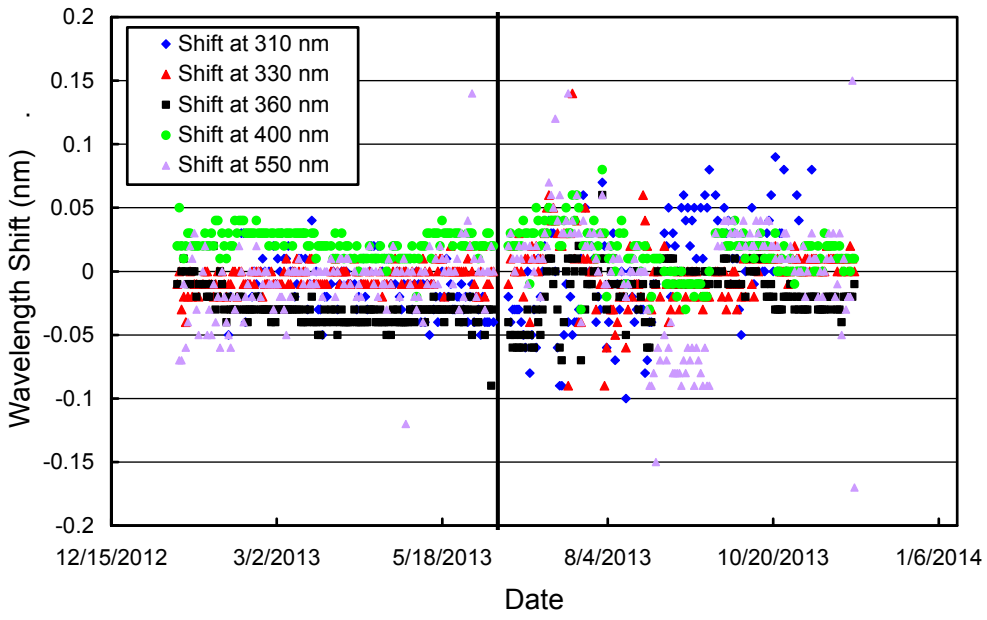

Figure 5.6.9. *Wavelength accuracy check of final data at four wavelengths in the UV and one in the visible by means of Fraunhofer-line correlation. The noontime measurement has been evaluated for each day of the reporting period when the Sun was above the horizon. The vertical black line marks the time of the site visit.*

5.6.4. Missing Data

A total of 14,056 scans are part of the Barrow Volume 23 dataset (01/13/13 – 11/28/13). There are no data for the following periods:

- 03/26/13: Raw data files were overwritten when GPS received updated system time incorrectly
- 06/14/13 - 06/15/13: Site visit
- 09/21/13 - 09/23/13 System software upgrades

5.6.5. GUV Data

The GUV-511 radiometer installed next to the SUV-100 was calibrated against final SUV-100 measurements following the procedure outlined in Section 4.3.1. Data products were calculated from calibrated measurements (Section 4.3.2). Figure 5.6.10. shows a comparison of SUV-100 and GUV-511 erythemal irradiance based on final Volume 23 data. The bias between the two instruments depends somewhat on season. Some of the seasonality is caused by the simplifications of the GUV inversion procedure. Measurements of the GUV's 305 nm channel are close to the detection limit when SZA exceeds 75° and the total ozone column is large. The large noise in GUV data during those conditions also affects the calculation of secondary data products such as erythemal irradiance. We advise data users to use SUV-100 rather than GUV-511 data, in particular when the SZA exceeds 75°. For SZAs < 75°, the median ratio SUV/GUV is 1.023.

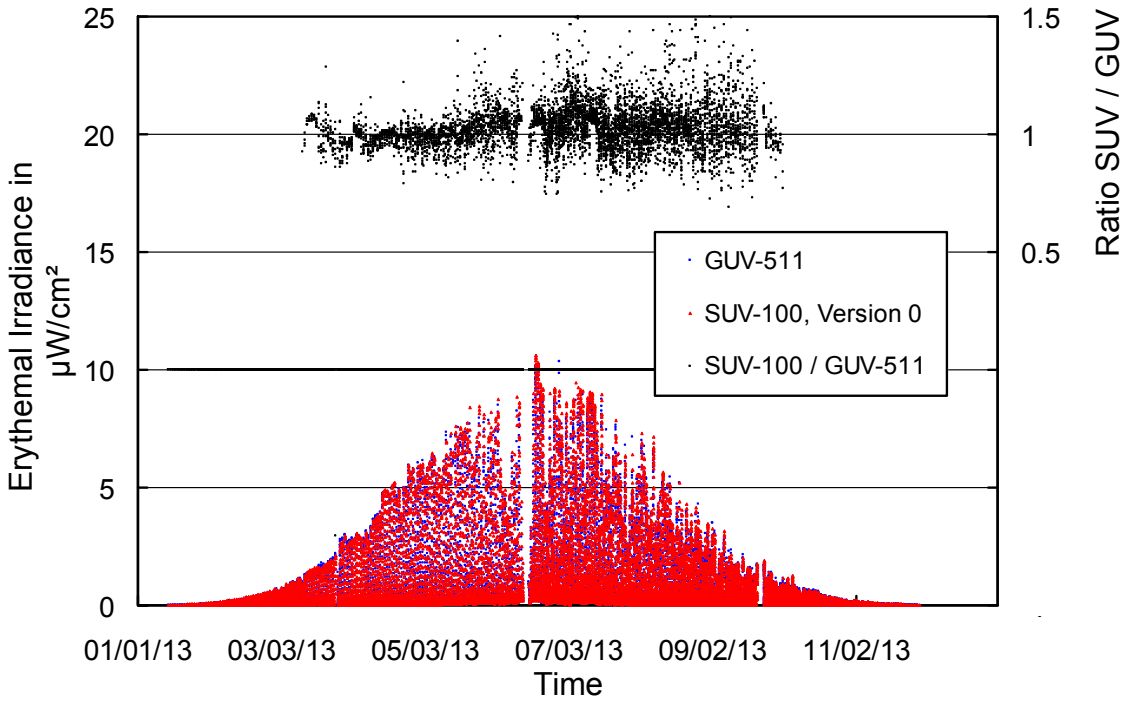

Figure 5.6.10. *Comparison of erythemal irradiance measured by the SUV-100 spectroradiometer and the GUV-511 radiometer. Data are based on "Version 0" (cosine-error uncorrected) data.*

Figure 5.6.11 shows a comparison of total ozone measurements from the GUV-511, the Ozone Monitoring Instrument (OMI) on NASA's AURA satellite (Version 8.5, Collection 3), and the SUV-100 (Version 2 data using climatological profiles with temperature correction). GUV-511 ozone values were calculated as described in Section 4.3.3. GUV-511 data measured between 4/15/13 and 9/28/13 are on average 1.5% larger than OMI observations. For SZAs larger than 75°, GUV-511 ozone data become unreliable and should not be used. SUV-100 ozone data exceed OMI measurements on average by 2.8%. For more information on total ozone calculation from SUV-data at Barrow see *Bernhard et al*. (2003). The effect of the vertical distribution of ozone has been further discussed by *Bernhard et al*. (2005).

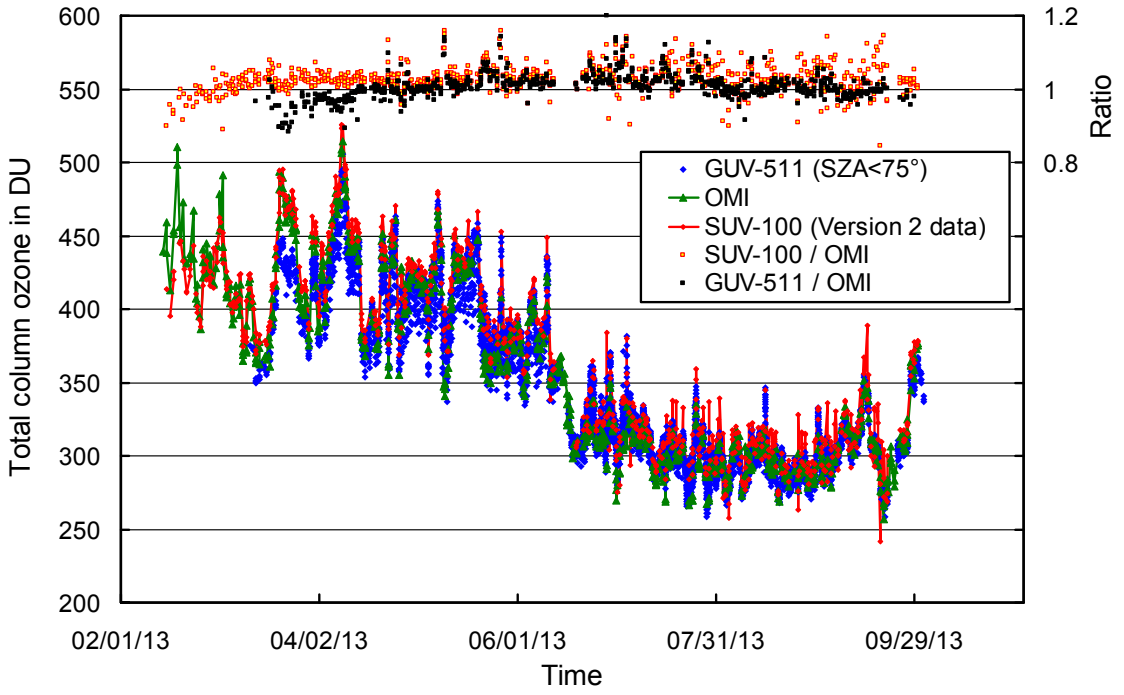

Figure 5.6.11. *Comparison of total column ozone measurements from GUV-511, OMI, and SUV-100. GUV-511 measurements are plotted in 30 minute intervals. For calculating the ratios of SUV-100/OMI and GUV-511/OMI, only measurements concurrent with the OMI overpass were evaluated.*

References

Bernhard, G., C.R. Booth, and R.D. McPeters. (2003). Calculation of total column ozone from global UV spectra at high latitudes. J. Geophys Research, 108(D17), 4532, doi:10.1029/2003JD003450.

Bernhard, G., C. R. Booth, and J. C. Ehramjian. (2004). Version 2 data of the National Science Foundation's Ultraviolet Radiation Monitoring Network: South Pole, J. Geophys. Res., 109, D21207, doi:10.1029/2004JD004937.

Bernhard, G., R.D. Evans, G.J. Labow, and S.J. Oltmans. (2005). Bias in Dobson Total Ozone Measurements at High Latitudes due to Approximations in Calculations of Ozone Absorption Coefficients and Airmass. J. Geophys. Res., 110, D10305, doi:10.1029/2004JD005559.

Bernhard, G., C. R. Booth, J. C. Ehramjian, R. Stone, and E. G. Dutton. (2007), Ultraviolet and visible radiation at Barrow, Alaska: Climatology and influencing factors on the basis of version 2 National Science Foundation network data, J. Geophys. Res., 112, D09101, doi:10.1029/2006JD007865.

Walker, J.H., R.D. Saunders, J.K. Jackson, and D.A. McSparron. (1987). Spectral Irradiance Calibrations. NBS Special Publication 250-20, U.S. Dept. of Commerce, National Bureau of Standards, Washington, DC, 37 pp., plus appendices.

Yoon H.W., C.E. Gibson, and P.Y. Barnes. (2002). Realization of the National Institute of Standards and Technology detector-based spectral irradiance scale. Appl. Opt., 41(28), 5,879-5,890.